



A Persistently Increasing Precipitation Trend Through the Holocene in Northwest China Recorded by Black Carbon $\delta^{13}\text{C}$ From Sayram Lake

Qingfeng Jiang^{1*}, Jianan Zheng¹, Yufeng Yang¹, Wenwei Zhao¹ and Dongliang Ning^{1,2}

¹ School of Geography Sciences, Nantong University, Nantong, China, ² State Key Laboratory of Lake Science and Environment, Nanjing Institute of Geography and Limnology, Chinese Academy of Sciences, Nanjing, China

OPEN ACCESS

Edited by:

Liangcheng Tan,
Chinese Academy of Sciences, China

Reviewed by:

Jianghu Lan,
Chinese Academy of Sciences, China

Yu Li,
Lanzhou University, China

*Correspondence:

Qingfeng Jiang
qfjiangz@163.com;
qfjiangz@ntu.edu.cn

Specialty section:

This article was submitted to
Quaternary Science, Geomorphology
and Paleoenvironment,
a section of the journal
Frontiers in Earth Science

Received: 29 February 2020

Accepted: 27 May 2020

Published: 17 July 2020

Citation:

Jiang Q, Zheng J, Yang Y, Zhao W
and Ning D (2020) A Persistently
Increasing Precipitation Trend
Through the Holocene in Northwest
China Recorded by Black Carbon
 $\delta^{13}\text{C}$ From Sayram Lake.
Front. Earth Sci. 8:228.
doi: 10.3389/feart.2020.00228

Precipitation is an important requirement for the stable and sustainable development of ecosystems and communities in arid areas, which are vulnerable to the influences of climate change. The changes in precipitation throughout the Holocene, as well as its long-term characteristics in arid northwest China, are not well understood, and records to reconstruct the precipitation trends are needed. Therefore, this study established a well-dated black carbon (BC) stable isotope-inferred ($\delta^{13}\text{C}$) precipitation record based on a sediment core from Sayram Lake, Tianshan Mountains (Xinjiang province, northwest China). The record spans the last 12880 cal. yr BP. Variations in BC $\delta^{13}\text{C}$ showed that between ~ 12280 and 9260 cal. yr BP, regional precipitation gradually decreased, but then increased continually until the present, with millennial to centennial scale fluctuations. During the Holocene, a distinct period of low precipitation was observed between 9800 and 8800 cal. yr BP, and two episodes of high precipitation were observed between 8000 and 7600, and 5800 and 2500 cal. yr BP. The maximum precipitation occurred at ~ 3800 cal. yr BP. Generally, the persistently increasing precipitation trend is consistent with other records from arid northwest China and adjacent areas. The trend was possibly controlled by Northern Hemisphere solar insolation and associated substantial ice sheet remnants, due to the influence of the North Atlantic Ocean sea surface temperatures and intensities of the Westerlies, which regulate the transport of water vapor to Xinjiang. The results provide a better understanding of the mechanisms driving the evolution of precipitation through the Holocene.

Keywords: black carbon isotope, northwest China, precipitation, Holocene, Sayram Lake

INTRODUCTION

Northwest China is a vast territory characterized by an arid climate and fragile ecosystem (Chen et al., 2008). To maintain such a fragile regional ecosystem and ensure the sustainable development of human communities in these areas, water is a crucial factor. Precipitation, which has significantly affected the evolution of human civilizations, is one of the most important sources

of water in northwest China (Zhao et al., 1995). Considering the impact of potential changes to water availability on ecosystems and societies, it is important to assess their vulnerability to predicted warming of the climate. For such an assessment, understanding the evolution of regional precipitation over a historical period is necessary (Swann et al., 2018). Meteorological observations from northwest China, however, have been recorded over a duration that is too short to evaluate the evolution of precipitation over different timescales, or to predict future changes. Therefore, to provide a scientific basis for understanding regional water availability in response to future climate warming, over the past two decades, geological archives have been used to reconstruct the long-term evolution of precipitation/moisture in the region. Examples of such geological archives include: cave stalagmites (Cheng et al., 2012, 2016; Cai et al., 2017), desert sand dunes (Ran and Feng, 2014; Long et al., 2017), loess deposits (Chen et al., 2016; Xie et al., 2018), tree rings (Gou et al., 2015; Deng et al., 2016, 2017; Yang et al., 2019), lake sediments (Jiang et al., 2007, 2013; Liu et al., 2008; An et al., 2011; Li et al., 2011; Wang W. et al., 2013; Huang et al., 2015, 2018; Zhao et al., 2015, 2018), ice cores (Thompson et al., 1997, 2018), and peat deposits (Zhang and Feng, 2018; Xu et al., 2019). However, the results of these studies are contradictory with regard to the evolution of precipitation/moisture (Chen et al., 2008; Long et al., 2017). For example, arboreal pollen abundances from Bosten Lake, which are indicative of the moisture level in the lake catchment area, indicated that the Holocene climate was the wettest during 8–6 ka (Tarasov et al., 2019), whereas abundances of *Ephedra* from the same area and same elevation range suggested that the climate was relatively dry throughout the Holocene (Huang et al., 2009). As another example, a profile of the Big Black Peatland in the Southern Altay Mountains showed the middle Holocene to be dry, while a profile of the Kelashizi Peat, only 140 km away, showed a wet middle Holocene (Wang and Zhang, 2019; Xu et al., 2019). The reasons for these different understandings and interpretations of the same climate proxy are unclear. Similarly, the proposed mechanisms, as well as the sensitivity of indexes, that reflect responses to precipitation are inconsistent. Thus, more records on precipitation variation are needed to deepen our understanding of regional Holocene moisture changes, as well as the associated mechanisms.

Black carbon (BC) is a product of the incomplete combustion and pyrolysis of biomass and fossil fuels. It includes a series of carbonaceous materials with different degrees of carbonization, such as charcoal, carbon chips, graphite carbon, and soot (Masiello, 2004; Bird and Ascough, 2012). Owing to its chemical stability, including a strong resistance to oxidation and decomposition, it can remain unchanged in soil, and in ocean, lake, and other sediments for a long time. Recently, the stable isotope, $\delta^{13}\text{C}_{\text{BC}}$, which is present in the BC in lake sediments, has been extensively used in the reconstruction of paleofires, paleovegetations, paleoclimates, and paleoenvironments. This is because it can trace and provide information on the features of burned plants and their surrounding climatic and environmental conditions (Bird and Gröcke, 1997; Wang X. et al., 2013; Sun et al., 2015, 2017; Zhang et al., 2015; Zhang E. et al., 2018).

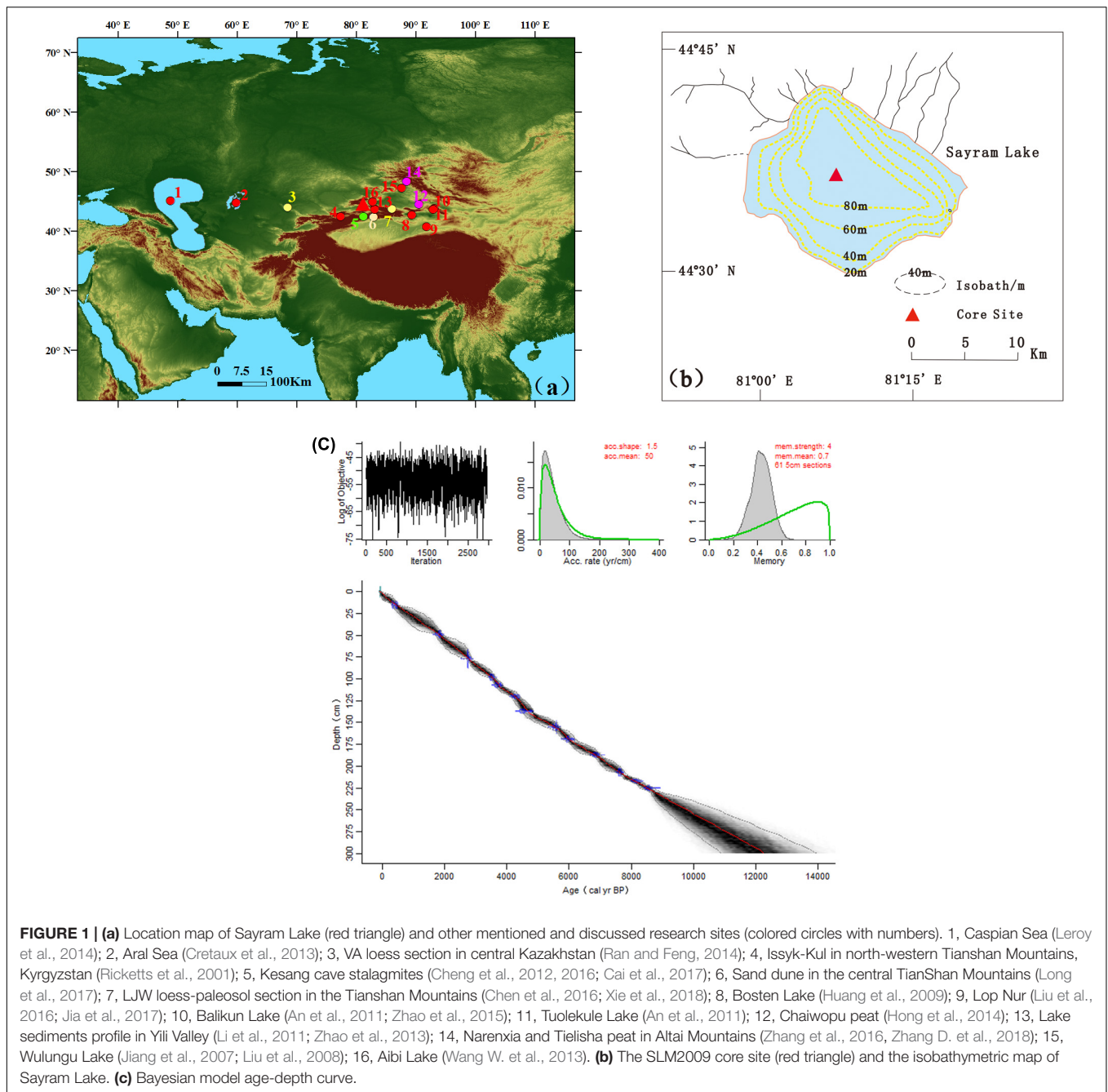
To enable the reconstruction of the evolution of regional precipitation, this study will generate a well-dated BC stable isotope-inferred precipitation record using Holocene sediments from Sayram Lake in arid northwest China. The record will be compared with published Holocene precipitation data from the study area as well as from adjacent areas, to identify potential correlations and understand possible driving mechanisms for climate change on millennial to centennial scales.

STUDY SITE

Sayram Lake (44°30′–44°42′ N, 81°05′–81°15′ E, 2071.9 m a.s.l.) is located on the western side of the Tianshan Mountains in Xinjiang province, northwest China. It is a vast closed alpine lake (Figure 1a) that is approximately elliptical (30 km long from east to west, and 27 km wide from north to south) (Figure 1b). It covers a total area of 453.0 km² and its catchment has a total area of 1408 km² (Wang and Dou, 1998). The lake has a storage capacity of $261 \times 10^8 \text{ m}^3$ and in 2012 its maximum and average water depths were 99 and 56 m, respectively (Wu et al., 2012).

The Sayram Lake area, climate within the Eurasian continental temperate zone, is characterized by a continental semi-arid. It freezes in late October, and remains frozen (ice thickness: 0.7–1.1 m) for ~150 days (i.e., from October to early May) (Wang and Dou, 1998). According to observational data collected during 1958–2018 from the nearest Wenquan County meteorological station (~30 km away, and 1354.6 m a.s.l.), the annual average temperature and precipitation were ~3.9°C and ~236 mm, respectively. About 80% of precipitation (primarily derived from water vapor carried by westerly circulation) occurs between May and September (Zhang and Deng, 1987; Aizen et al., 2001). Between October and April, precipitation primarily results from the Siberian anticyclone, which accounts for <20% of the mean annual precipitation (Zhang and Deng, 1987; Aizen et al., 2001).

Water supply into Sayram Lake primarily results from precipitation, groundwater flow, and melted ice and snow. Thirty-two rivers (predominantly distributed along the western and northwestern lake margins) drain into the lake (Hu, 2004). Among the rivers, seven are perennial and the others are seasonal. Sagakele River is the largest river (18.0 km long) and the only river that flows directly into the lake. Its average annual runoff is $\sim 0.24 \times 10^8 \text{ m}^3$, which mainly results from precipitation. The other rivers recharge the lake via surface runoff or groundwater flow, with an inflow of $\sim 0.68 \times 10^8 \text{ m}^3$. Surface precipitation into the lake is $\sim 1.6 \times 10^8 \text{ m}^3$, and accounts for 63% of the total lake water recharge. Water loss from the lake is primarily due to evaporation on the lake surface, with an average annual evaporation of 550.0 mm (Wang and Dou, 1998) and total annual evaporation of $2.49 \times 10^8 \text{ m}^3$. Presently, annual inflow is $\sim 2.52 \times 10^8 \text{ m}^3$, and there is an approximate balance between inflow and outflow (Wang and Dou, 1998). Additionally, the glacier area in the Sayram Lake basin is small, i.e., $\sim 4.28 \text{ km}^2$ (Hu, 2004). It only accounts for ~0.3% of the total basin area. Thus, the impact of glacial melt water on surface runoff and lake water level/area may be negligible (Lan et al., 2019).



MATERIALS AND METHODS

In July 2009, a 300-cm long sedimentary core was extracted from the center of Sayram Lake (Figure 1b, SLMH2009, 44°34'59.0'' N, 81°09'12.3'' E) at a depth of 86.0 m using a piston corer attached to a UWITEC drilling platform. After extraction, the sediment core was transported to the laboratory, where it was cut longitudinally, and sampled at 1-cm intervals. The samples were then stored in a refrigerator at 4°C until analysis.

To establish the sedimentary chronology, the accelerator mass spectrometry (AMS) ¹⁴C dating method was used.

Without any suitable terrestrial plant residues, only bulk organic matter in the lake sediments was used for dating. Fourteen samples from different depths along the core were dated. The dating analyses were performed by the AMS Laboratory of Tokyo University (Japan) and by the Beta Analytic Radiocarbon Dating Laboratory in Miami (United States). All AMS ¹⁴C dates, of which twelve had been previously reported by Jiang et al. (2013), were calibrated to calendar years using the Calib 7.1 program under the IntCal13 model (Reimer et al., 2013). Additionally, an age-depth curve was derived using the Bayesian model in the

Bacon 2.2 program in R v3.4.4 (Blaauw and Christen, 2011; R Development Core Team, 2013).

For $\delta^{13}\text{C}_{\text{BC}}$ analyses, 150 samples of bulk sediment were collected at 2-cm intervals. To extract and isolate BC from the lake sediments, the chemical oxidation method developed by Lim and Cachier (1996) was used. About 1.0 g of the dry powder bulk sediment was weighed. Carbonates and some of the silicates were removed via treatment with HCl (3 mol/L), HF (10 mol/L), HCl (1 mol/L), and HCl (3 mol/L) in sequence. To completely remove kerogen and soluble organic matter, $\text{K}_2\text{Cr}_2\text{O}_7$ (0.2 mol/L) and H_2SO_4 (2 mol/L) were added to oxidize the acid-treated samples (60 h, 55°C). After treatment, refractory carbon in the sediment was considered to be BC, which represents charcoal and soot resulting from regional fires and other earlier sources (Lim and Cachier, 1996). Determination of $\delta^{13}\text{C}_{\text{BC}}$ was performed by the State Key Laboratory of Lake Science and Environment, Nanjing Institute of Geography and Limnology, Chinese Academy of Sciences using a Thermo Delta V Advantage isotope mass spectrometer coupled with a Flash EA 1112 element analyzer. The $\delta^{13}\text{C}_{\text{BC}}$ values obtained were expressed using the delta per mil (δ , ‰) notation relative to Vienna Pee Dee Belemnite (V-PDB) as a standard. The accuracy of isotopic analyses was calibrated and evaluated based on replicate measurements using standard laboratory materials, and an accuracy of greater than $\pm 0.2\%$ was obtained.

RESULTS

Table 1 shows the dating results of the 14 sediment samples. One sample, S1m1-245, diverged from the age-depth line that fits the other dates and has been excluded from the chronology of Sayram Lake. Lakes with carbonates in their basin can be affected by the “reservoir” effect, which is caused by the mixing of “old carbon” from the bedrock. There is usually uncertainty in age-depth models established using radiocarbon dates of bulk organic matter samples from such lakes (Hou et al., 2012). Generally, the “reservoir” effect is considered as the difference between zero and the age at the sediment-water interface obtained via linear extrapolation of the age-depth curve. The carbon reservoir age of the Sayram Lake was inferred to be 778a (**Figure 1c** and **Table 1**). This is approximately equal to the difference ($\sim 800\text{a}$) between AMS^{14}C and ^{137}Cs dating results at a core depth of 15 cm (**Supplementary Figures 1–3**). Even though this estimation for the late Holocene radiocarbon reservoir effect is slightly smaller than that proposed by Lan et al. (2019) (1073a), which could be attributed to the estimations being made at different times, it is still close to the reservoir effect estimated for other lakes in Xinjiang province, including Wulungu Lake (760a, Liu et al., 2008), Balikun Lake (790a, An et al., 2011), and Bosten Lake (200–1140a, Huang, 2006). Therefore, the reservoir-corrected estimation of 778a was considered reliable. After subtracting 778a from the final age-depth model presented in **Figure 1c**, the 13 reliable dating results were converted to calendar years. The mean weighted age at the base of the SLMH2009 core was found to be ~ 12280 cal. yr BP, and the sedimentation rate through the core

was between 0.17–0.34 cm/yr. With an average sedimentation rate of 0.26 cm/yr, the average resolution of the $\delta^{13}\text{C}_{\text{BC}}$ record from Sayram Lake was ~ 50 yr.

The $\delta^{13}\text{C}_{\text{BC}}$ values ranged from -30.9 to -22.1% , with a mean of -27.4% (**Figure 2a**). The general variation in $\delta^{13}\text{C}_{\text{BC}}$ could be roughly divided into three stages: Stage 1, 12280–9260 cal. yr BP, during which $\delta^{13}\text{C}_{\text{BC}}$ increased from -26.9 to -22.1% , with a mean of -25.0% ; Stage 2, 9260–8000 cal. yr BP, during which $\delta^{13}\text{C}_{\text{BC}}$ decreased abruptly from -22.1 to -30.4% ; and Stage 3, 8000 cal. yr BP to present, during which $\delta^{13}\text{C}_{\text{BC}}$ increased from -30.9 to -26.8% , with a mean of -28.1% . These overall $\delta^{13}\text{C}_{\text{BC}}$ trends were punctuated by several millennial-scale excursions, which included $\delta^{13}\text{C}_{\text{BC}}$ enrichments centered at 9200 and 7400 cal. yr BP, and depletions at ~ 8000 – 7600 and 5800 – 2500 cal. yr BP.

DISCUSSION

Interpretation of the $\delta^{13}\text{C}_{\text{BC}}$ in Sayram Lake

Studies have demonstrated that $\delta^{13}\text{C}_{\text{BC}}$ can be influenced by several factors (Bird and Ascough, 2012), including the stable carbon isotope compositions of the burned precursors (e.g., Street-Perrott et al., 1997; Huang et al., 2001; Zhang et al., 2003), relative abundances of different burned plant species (e.g., Wang X. et al., 2013; Sun et al., 2015, 2017; Zhang et al., 2015), isotope fractionation during pyrolysis, and modification that occurs during diagenesis (e.g., Bird and Ascough, 2012; Sun et al., 2015, 2017).

During photosynthesis, the $\delta^{13}\text{C}$ values of terrestrial plants can be modified via carbon isotope fractionation, and plants can be classified into three types depending on their carbon-fixation pathways: C_3 , C_4 , and CAM plants (O’Leary, 1981, 1988). The C_3 plants, which include trees, most shrubs and grasses, and sedges, are characterized by the C_3 carbon-fixation pathway under cold climatic conditions, and their $\delta^{13}\text{C}$ values range from -34 to -20% , with a mean of -27% (Bird et al., 1996). The C_4 plants, which include most grasses and sedges, are characterized by the C_4 carbon-fixation pathway under warm climatic conditions, and their $\delta^{13}\text{C}$ values are relatively higher, and range between approximately -16 to -10% , with a mean of -13% (Smith and Epstein, 1971; O’Leary, 1981; Farquhar et al., 1989). The CAM plants, which include most succulents, and can survive in extremely dry environments, are characterized by both the C_3 and C_4 carbon-fixation pathways, and they have a large range of $\delta^{13}\text{C}$ values, from -28% to -11% (O’Leary, 1988; Lüttge, 2004).

Carbon isotope fractionation of plants during pyrolysis to BC varies with pyrolysis temperature and the amount of oxygen available. It also varies with the proportion of carbon components as well as the isotopic composition of different plant tissues (Sun et al., 2017). Most pyrolysis experiments have confirmed that the variation of plant carbon-isotope fractionation during pyrolysis is in the range of 1–2%, with an average carbon-isotope depletion of 0.3 and 1.7% for C_3 and C_4 plants, respectively (Bird and Gröcke, 1997; Bird and Ascough, 2012; Wang X. et al., 2013).

TABLE 1 | AMS ^{14}C dating results.

Sample number	Laboratory I.D.	Depth/cm	Dating material	^{14}C age/aBP	$\delta^{13}\text{C}/\%$	C/N	Reservoir-corrected ^{14}C age by 778a	Calendar age/cal. yr BP(2 σ)
Slm1-15	Tka-15142	14–15	TOC	1150 \pm 25	–25.7	13.4	372	426–501 (464)
Slm1-49	Tka-15163	48–49	TOC	2670 \pm 35	–26.3	14.9	1892	1727–1899 (1813)
Slm1-77	Tka-15143	76–77	TOC	3425 \pm 30	–27.6	14.0	2647	2739–2796 (2768)
Slm1-98	Beta469443	97–98	TOC	4080 \pm 30	–27.1	15.4	3302	3454–359 (3524)
Slm1-107	Tka-15144	106–107	TOC	4215 \pm 35	–29.6	18.1	3437	3608–3780 (3694)
Slm1-120	Beta469444	119–120	TOC	4640 \pm 30	–26.5	13.7	3862	4225–4411 (4318)
Slm1-137	Tka-15164	136–137	TOC	4815 \pm 45	–28.9	12.9	4037	4416–4629 (4523)
Slm1-155	Tka-15145	154–155	TOC	5625 \pm 35	–28.7	15.4	4847	5578–5651 (5615)
Slm1-169	Tka-15165	168–169	TOC	5980 \pm 45	–25.4	17.2	5202	5893–6029 (5961)
Slm1-187	Tka-15146	186–187	TOC	6795 \pm 35	–26.8	12.0	6017	6776–6949 (6863)
Slm1-207	Tka-15147	206–207	TOC	7555 \pm 40	–28.0	10.5	6777	7577–7677 (7627)
Slm1-217	Tka-15166	216–217	TOC	8120 \pm 50	–25.2	14.6	7342	8021–8220 (8121)
Slm1-225	Tka-15148	224–225	TOC	8560 \pm 45	–26.7	10.3	7782	8455–8639 (8542)
Slm1-245	Tka-15149	244–245	TOC	14550 \pm 60	–18.2	4.2	/	/

Black carbon is usually considered stable, and remains unchanged after deposition (Bird and Ascough, 2012), especially if buried in low-temperature and non-oxidizing environments. Due to the relatively high altitude, relatively deep, low temperature, and anoxic bottom of Sayram Lake, post-depositional modification of the isotopes in BC was considered negligible. Thus, the $\delta^{13}\text{C}_{\text{BC}}$ values of the lake sediment samples were primarily determined by the variation in C_3 and C_4 terrestrial plants inhabiting the area, as well as the variation of their proportions during combustion. This means that $\delta^{13}\text{C}_{\text{BC}}$ values are generally indicative of the regional paleovegetation in a given area (Bird and Gröcke, 1997; Bird and Cali, 1998; Clark et al., 2001; Jia et al., 2003; Sun et al., 2015; Zhang et al., 2015). The $\delta^{13}\text{C}_{\text{BC}}$ values for Sayram Lake were less than -27% , suggesting that over the past ~ 12280 yr, the lake basin and surrounding region were predominantly inhabited by C_3 plants. This is consistent with the findings from loess areas of Xinjiang, which also suggested that arid northwest China was mainly inhabited by C_3 plants throughout the Holocene (Xie et al., 2018).

During photosynthesis in C_3 plants, climatic factors including temperature, precipitation, and atmospheric CO_2 concentration, as well as vital effects, directly affect the fractionation of carbon isotopes (Sage et al., 1999; Kohn, 2010). Globally, there is a significant negative correlation between $\delta^{13}\text{C}$ and mean annual precipitation. Furthermore, for C_3 plants, the correlation between $\delta^{13}\text{C}$ and mean annual precipitation is much more significant than that between $\delta^{13}\text{C}$ and mean annual temperature (Rao et al., 2017). This has been confirmed by studies on the Loess Plateau in China, which showed that the $\delta^{13}\text{C}$ of C_3 plants generally increased with decreasing precipitation (Wang et al., 2008, 2018). The atmospheric CO_2 concentration was generally stable during the Holocene (Monnin et al., 2004), and its effects on carbon-isotope fractionation in C_3 plants were considered negligible (Schubert and Jahren, 2012). Even though these factors are uncertain for the Sayram Lake area, the $\delta^{13}\text{C}_{\text{BC}}$ values of the Sayram Lake sediment samples can be used as a paleo-precipitation

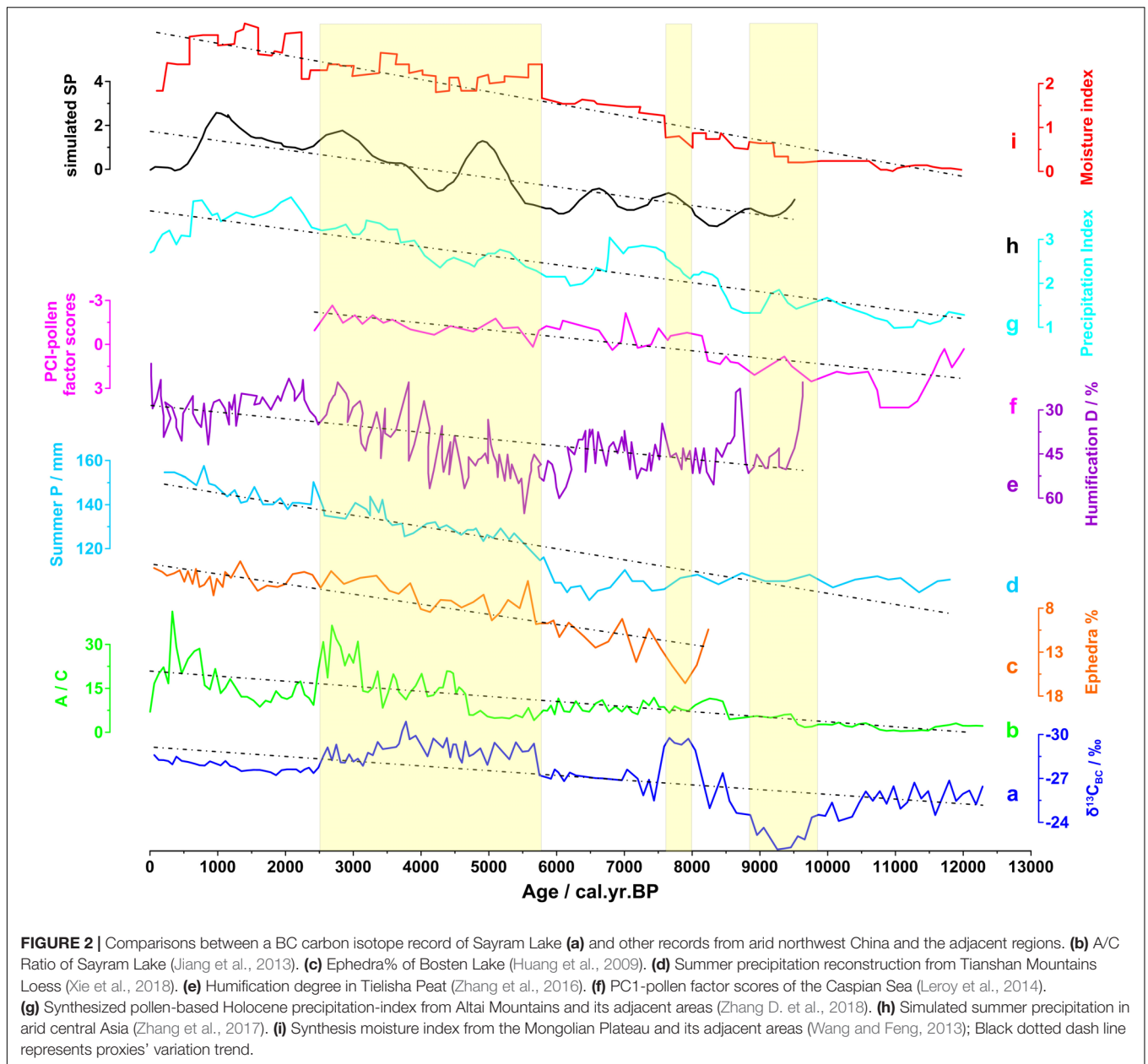
proxy, with more positive $\delta^{13}\text{C}_{\text{BC}}$ values indicating lower precipitation, and vice versa.

The relationship between BC isotope composition and climate factors, such as precipitation and temperature in the study area, had not been investigated. However, studies on the correlation between climate factors and the carbon isotopes in modern plants, as well as topsoil organic matter in the Tianshan Mountains (**Supplementary Figures 4–9**), have shown that the organic carbon isotope composition of modern plants and topsoil organic matter are strongly negatively correlated with precipitation, and weakly positively correlated with temperature. These relationships were stronger when only the isotope compositions of samples from the northern slope of the Tianshan Mountains, where Sayram Lake is located, were considered. These findings establish precipitation as a key factor that controls the organic carbon isotope composition in modern plants and topsoil organic matter. Most importantly, BC isotopes can be used as an alternative indicator of precipitation and its evolution in an area.

Variations of Holocene Precipitation in Northwest China

The variation of $\delta^{13}\text{C}_{\text{BC}}$ from ~ 12280 to 9260 cal. yr BP revealed a gradual decrease in precipitation in the study area. Thereafter, it increased persistently through the Holocene with millennial- to centennial-scale fluctuations superimposed (**Figure 2a**). A distinct low-precipitation episode appeared between 9800 and 8800 cal. yr BP, with the lowest precipitation at 9260 cal. yr BP. Two high precipitation episodes were also observed between 8000 and 7600, and 5800 and 2500 cal. yr BP, and the highest precipitation was observed at ~ 3800 cal. yr BP.

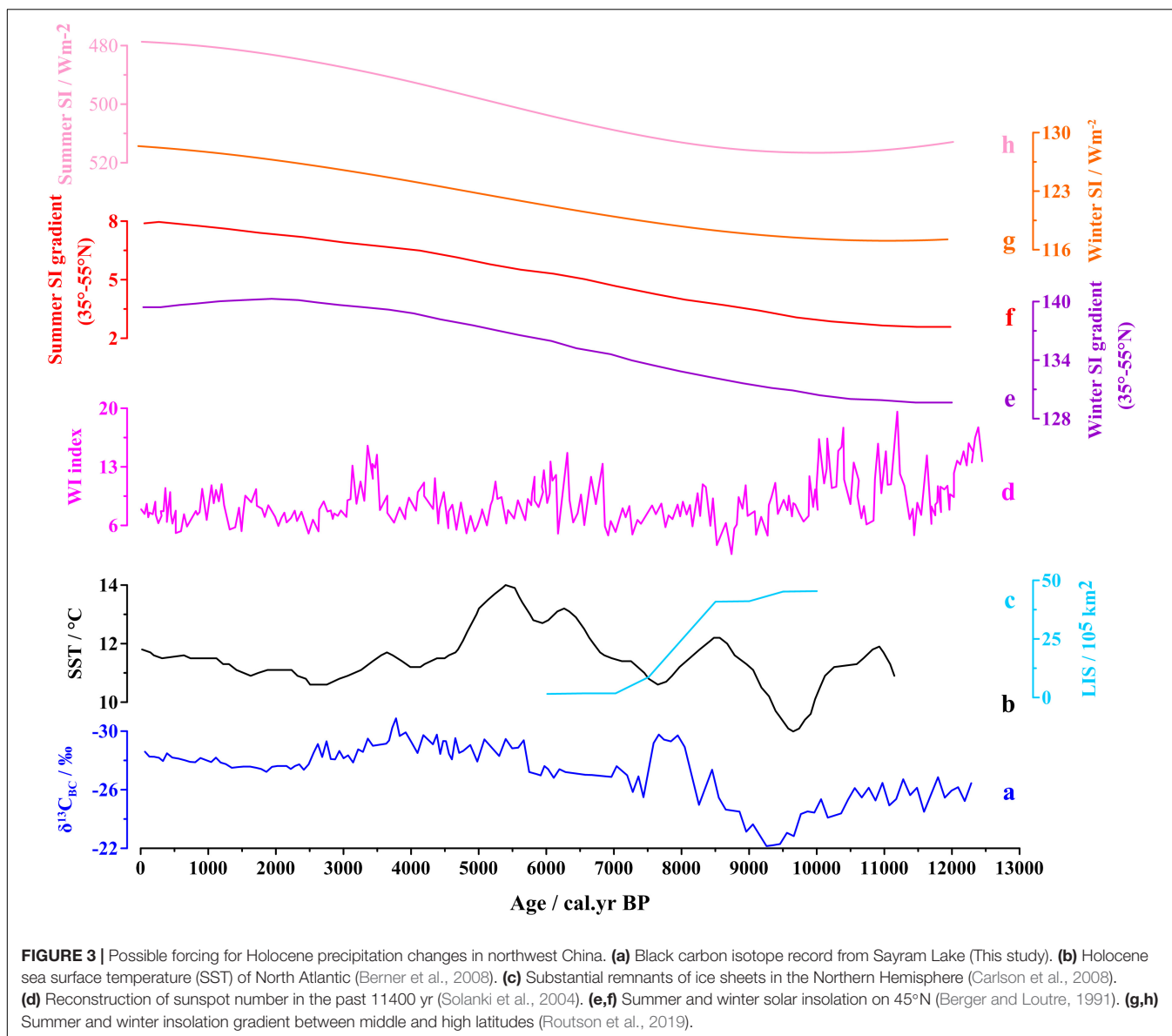
The gradually decreasing and increasing precipitation trends before and after 9260 cal. yr BP, respectively, based on the $\delta^{13}\text{C}_{\text{BC}}$ data from Sayram Lake, were found to be consistent with the moisture changes reconstructed using *Artemisia* and *Chenopodiaceae* pollen percentage ratios (i.e., A/C, **Figure 2b**) from the same sediment core (Jiang et al., 2013). However,



there were also some differences between the precipitation and moisture levels recorded in this study and those reported in previous studies. Jiang et al. (2013) reported that precipitation increased sharply during the early Holocene, while moisture levels increased at a relatively slower pace. This difference could be attributed to the higher evaporation rate caused by higher temperature instability during this period.

Variations in $\delta^{13}\text{C}_{\text{BC}}$ -inferred Holocene precipitation observed in this study generally resemble those observed in other lake sediment records from adjacent regions in northwest China. Even though characterized by significant fluctuations, similar moisture evolution trends have been observed in Bosten, Wulungur, and Swan Lake based on *Ephedra* abundance, A/C ratios, and Cyperaceae/Poaceae ratios, respectively, as shown in

Figure 2c (Jiang et al., 2007; Liu et al., 2008; Huang et al., 2009, 2015). The principle component 1 values of pollen abundance and carbonate content in sediments from Balikun Lake showed a moisture threshold at ~ 8000 cal. yr BP, which increased rapidly for a short while, and thereafter decreased slowly, accompanied by significant fluctuations. The studies on Balikun Lake showed a very wet late Holocene period (An et al., 2011; Zhao et al., 2015). Based on A/C ratios, moisture records from Aibi Lake sediments also showed a mildly dry early Holocene, a progressively wet middle Holocene, and a very wet late Holocene after 2000 cal. yr BP (Wang W. et al., 2013). The annual precipitation record from Kanas Lake reconstructed using a palynological transfer function also showed a continuously increasing Holocene wetness trend (Huang et al., 2018).



Moreover, other sedimentary records within arid northwest China also support the generally increasing precipitation pattern recorded in Sayram Lake. Holocene moisture variation based on magnetic parameters $\chi_{ARM}/SIRM$ from a loess-paleosol section in the Tianshan Mountains showed a continuously increasing humidity trend, with the wettest period during the late Holocene (Chen et al., 2016). An organic carbon isotope-based summer precipitation reconstruction from the same loess-paleosol profile also indicated an increasing precipitation trend throughout the Holocene (Figure 2d; Xie et al., 2018). Additionally, AP/NAP pollen ratios from Narenxia Peat (Altay Mountains), humification degree data from Tielisha Peat (Altay Mountains), and $\delta^{13}C$ value of α -cellulose from Chaiwopu Peat (eastern Tianshan Mountains) also showed gradually increasing Holocene moisture trends with large fluctuations (Figure 2e; Hong et al., 2014; Zhang et al., 2016; Feng et al., 2017).

Records from studies outside the northwest China region also confirm a persistently increasing precipitation trend in arid areas during the Holocene. Organic carbon $\delta^{13}C$ from the VA loess section in Kazakhstan showed that the moisture level fluctuated along a constant line between early to mid-Holocene, and then increased during the last ca. 5000 yr (Ran and Feng, 2014). The principle component 1 scores based on pollen measurements from the Caspian Sea indicated that moisture levels increased consistently from 12440 to 2430 cal. yr BP (Figure 2f; Leroy et al., 2014). In addition to the pollen data, dinocyst assemblages from the Caspian Sea clearly revealed a 6000-yr long highstand sea level between 10550 and 4110 cal. yr BP, implying a higher precipitation/moisture level (Leroy et al., 2014).

The synthesized pollen-based Holocene precipitation-index for the lowland Altay Mountains and adjacent areas (Figure 2g; Zhang D. et al., 2018), the simulated summer precipitation

variations in arid central Asia (Figure 2h; Zhang et al., 2017), and the synthesized moisture index from the Mongolian Plateau and adjacent areas (Figure 2i; Wang and Feng, 2013) also indicated an increasing precipitation trend throughout the Holocene, even though since 1000 cal. yr BP it has been declining.

Notably, all the above-mentioned precipitation and moisture level records showed different precipitation rate and range changes. However, the general trend is for gradually decreasing precipitation during the early Holocene, followed by a persistent increase in precipitation until the present. The trend is clear even though the proxy records are possibly affected by age uncertainties, regional climate differences, and the impacts of a variety of climate factors (Liu et al., 2006; Rao et al., 2019).

Possible Forcing for Holocene Precipitation Changes in Northwest China

Modern observations and paleoclimate simulations have confirmed that water vapor originating from the North Atlantic Ocean, and the Mediterranean, Black, and Caspian Seas, and transported by Westerlies, represents the dominant moisture source that supplies precipitation to arid northwest China (Zhang and Deng, 1987; Aizen et al., 1997, 2001; Jin et al., 2012; Wang B.L. et al., 2013; Zhao et al., 2013; Huang et al., 2017; Xu et al., 2019). Therefore, sea surface temperatures (SST) of the North Atlantic Ocean and the intensity of the Westerlies are probably the primary factors that directly influence rainfall patterns in the study area. This inference is supported by the nearly synchronous Holocene evolution of the precipitation changes recorded in Sayram Lake and changes in the intensity of the Westerlies recorded in the Tianshan Mountains (Jia et al., 2018), Qinghai Lake (An et al., 2012), and SST data from the North Atlantic Ocean (Berner et al., 2008).

Previous studies have shown that solar insolation in the Northern Hemisphere is the main factor that controls the intensity of Westerlies (Jin et al., 2012). The winter and summer insolation at mid-latitudes increase and decrease, respectively, faster than that at high latitudes; the insolation gradient between the middle and high latitudes has increased gradually from the early Holocene period onward (Figure 3; Jin et al., 2012; Routson et al., 2019). This increased insolation gradient possibly results in more intense Westerlies (Routson et al., 2019), which could have potentially transported more moisture from the North Atlantic Ocean to northwestern China, bringing about the increase in precipitation during the Holocene.

Additionally, both Northern Hemisphere solar insolation and the substantial ice sheet remnants, including the Laurentide and Fennoscandian ice sheets (Peltier and Fairbanks, 2006; Carlson et al., 2008), can significantly influence SSTs of the North Atlantic Ocean (Chen et al., 2016; He et al., 2017). Increasing winter insolation during the Holocene could have possibly warmed the sea surface, thereby enhancing evaporation over the North Atlantic Ocean (Chen et al., 2016). Thus, both the strengthened Westerly wind and the increased evaporation could have increased the moisture supply to northwestern China, leading to a wetter winter climate through the Holocene (Chen

et al., 2016). The corresponding decreasing summer insolation possibly resulted in the decreasing summer precipitation in northwestern China. However, a higher summer temperature during the early Holocene would have increased the melting of ice sheets, resulting in their expansion over the North Atlantic Ocean (Figure 3). This probably slowed down the Atlantic Meridional overturning circulation and reduced thermal transport from the equator to the middle and high latitudes, resulting in decreases in SSTs (McManus et al., 2004). As the Northern Hemisphere ice sheets gradually diminished, SST increased; coupled with more intense Westerlies, much more vapor was transported to northwest China, resulting in a persistently wet summer climate. Furthermore, a higher summer temperature resulting from higher summer insolation during the early Holocene could have caused northward displacement of the subtropical high, which inhibits precipitation development in northwest China (Chen et al., 2016). As summer temperatures decreased from the middle to late Holocene, the subtropical high could have migrated southward, leading to higher precipitation in this area. The enhanced precipitation in both summer and winter probably resulted in the increasing precipitation trend observed in the Sayram Lake area.

It is suggested that the persistently increasing precipitation trend observed in northwest China during the Holocene resulted from changes in Northern Hemisphere solar insolation and the substantial ice sheet remnants due to the influence of North Atlantic Ocean SSTs and increased intensity of the Westerlies.

CONCLUSION

In this study, to illustrate Holocene precipitation variation in arid northwest China, a BC isotope-inferred precipitation record of an alpine lake in the Tianshan Mountains in Xinjiang was presented. The chronology of the studied lake sediment core, which had a mean basal age of ~ 12280 years, was established using 13 AMS ^{14}C dates. The $\delta^{13}\text{C}_{\text{BC}}$ record showed that precipitation decreased between ~ 12280 and 9260 cal. yr BP, and then increased during the mid- to late Holocene. The reliability of the $\delta^{13}\text{C}_{\text{BC}}$ record, particularly the persistently increasing precipitation trend throughout the Holocene, was further supported by published precipitation and moisture records from northwest China and surrounding regions. It was inferred that the evolution of precipitation in arid northwest China throughout the Holocene was linked to Northern Hemisphere solar insolation and the substantial ice sheet remnants due to the influence of North Atlantic Ocean SSTs and the intensity of the Westerlies. Considering the importance of understanding the Holocene evolution of regional precipitation, as well as its driving mechanisms in arid areas, more reliable Holocene precipitation reconstructions are needed for further study.

DATA AVAILABILITY STATEMENT

The datasets generated for this study are available on request to the corresponding author.

AUTHOR CONTRIBUTIONS

QJ designed the research. QJ, JZ, YY, WZ, and DN performed the research. QJ, JZ, and YY analyzed the data. QJ, WZ, and DN wrote the manuscript. All authors contributed to the article and approved the submitted version.

FUNDING

This study was supported by the National Natural Science Foundation of China (Grant Nos. 41672349 and 40802084).

REFERENCES

- Aizen, E. M., Aizen, V. B., Melack, J. M., Nakamura, T., and Ohta, T. (2001). Precipitation and atmospheric circulation patterns at mid-latitudes of Asia. *Int. J. Climatol.* 21, 535–556. doi: 10.1002/joc.626
- Aizen, V. B., Aizen, E. M., Melack, J. M., and Dozier, J. (1997). Climatic and hydrologic changes in the Tien shan, Central Asia. *J. Climate* 10, 1393–1404. doi: 10.1175/1520-0442(1997)010<1393:cahcit>2.0.co;2
- An, C. B., Zhao, J. J., Tao, S. C., Lv, Y. B., Dong, W. M., Li, H., et al. (2011). Dust variation recorded by lacustrine sediments from arid Central Asia since similar to 15 cal ka BP and its implication for atmospheric circulation. *Quat. Res.* 75, 566–573. doi: 10.1016/j.yqres.2010.12.015
- An, Z., Colman, S. M., Zhou, W., Li, X., Brown, E. T., Jull, A. J., et al. (2012). Interplay between the Westerlies and Asian monsoon recorded in Lake Qinghai sediments since 32 ka. *Sci. Rep.* 2:619. doi: 10.1038/srep00619
- Berger, A., and Loutre, M. F. (1991). Insolation values for the climate of the last 10 million years. *Quat. Sci. Rev.* 10, 297–317. doi: 10.1016/0277-3791(91)90033-q
- Berner, K. S., Koc, N., Divine, D., Godtliebsen, F., and Moros, M. (2008). A decadal-scale Holocene sea surface temperature record from the subpolar North Atlantic constructed using diatoms and statistics and its relation to other climate parameters. *Paleoceanography* 23, 2211–2215. doi: 10.1029/2006pa001339
- Bird, M. I., and Ascough, P. L. (2012). Isotopes in pyrogenic carbon: a review. *Org. Geochem.* 42, 1529–1539. doi: 10.1016/j.orggeochem.2010.09.005
- Bird, M. I., and Cali, J. A. (1998). A million-year record of fire in sub-Saharan Africa. *Nature* 394, 767–769. doi: 10.1038/29507
- Bird, M. I., Chivas, A. R., and Head, J. (1996). A latitudinal gradient in carbon turnover times in forest soils. *Nature* 381, 143–146. doi: 10.1038/381143a0
- Bird, M. I., and Gröcke, D. R. (1997). Determination of the abundance and carbon isotope composition of elemental carbon in sediments. *Geochim. Cosmochim. Acta* 61, 3413–3423. doi: 10.1016/s0016-7037(97)00157-9
- Blaauw, M., and Christen, J. A. (2011). Flexible paleoclimate age-depth models using an autoregressive gamma process. *Bayesian Anal.* 6, 457–474. doi: 10.1214/11-ba618
- Cai, Y. J., Chiang, J. C. H., Breitenbach, S. F. M., Tan, L. C., Cheng, H., Edwards, R. L., et al. (2017). Holocene moisture changes in western China, Central Asia, inferred from stalagmites. *Quat. Sci. Rev.* 158, 15–28. doi: 10.1016/j.quascirev.2016.12.014
- Carlson, A. E., Legrande, A. N., Oppo, D. W., Came, R. E., Schmidt, G. A., Anslow, F. S., et al. (2008). Rapid early Holocene deglaciation of the Laurentide ice sheet. *Nat. Geosci.* 1, 620–624. doi: 10.1038/ngeo285
- Chen, F. H., Jia, J., Chen, J. H., Li, G. Q., Zhang, X. J., Xie, H. C., et al. (2016). A persistent Holocene wetting trend in arid central Asia, with wettest conditions in the late Holocene, revealed by multi-proxy analyses of loess-paleosol sequences in Xinjiang, China. *Quat. Sci. Rev.* 146, 134–146. doi: 10.1016/j.quascirev.2016.06.002
- Chen, F. H., Yu, Z. C., Yang, M. L., Ito, E., Wang, S. M., Madsen, D. B., et al. (2008). Holocene moisture evolution in arid central Asia and its out-of-phase relationship with Asian monsoon history. *Quat. Sci. Rev.* 27, 351–364. doi: 10.1016/j.quascirev.2007.10.017

ACKNOWLEDGMENTS

We thank the reviewers for their very valuable comments and suggestions. We also thank Dr. Chao Zhenhua and Dr. Zhou Tong from the School of Geography Sciences, Nantong University, for their assistance during field measurements.

SUPPLEMENTARY MATERIAL

The Supplementary Material for this article can be found online at: <https://www.frontiersin.org/articles/10.3389/feart.2020.00228/full#supplementary-material>

- Cheng, H., Spotl, C., Breitenbach, S. F., Sinha, A., Wassenburg, J. A., Jochum, K. P., et al. (2016). Climate variations of Central Asia on orbital to millennial timescales. *Sci. Rep.* 5:36975. doi: 10.1038/srep36975
- Cheng, H., Zhang, P. Z., Spotl, C., Edwards, R. L., Cai, Y. J., Zhang, D. Z., et al. (2012). The climatic cyclicity in semiarid-arid central Asia over the past 500,000 years. *Geophys. Res. Lett.* 39:L01705. doi: 10.1029/2011gl050202
- Clark, J. S., Grimm, E. C., Lynch, J., and Mueller, P. G. (2001). Effects of Holocene climate change on the C 4 grassland/woodland boundary in the Northern Plains, USA. *Ecology* 82, 620–636. doi: 10.2307/2680184
- Cretaux, J. F., Letolle, R., and Berge-Nguyen, M. (2013). History of Aral Sea level variability and current scientific debates. *Glob. Planet Change* 110, 99–113. doi: 10.1016/j.gloplacha.2013.05.006
- Deng, Y., Gou, X., Gao, L., Yang, M., and Zhang, F. (2016). Spatiotemporal drought variability of the eastern Tibetan Plateau during the last millennium. *Clim. Dynam.* 49, 2077–2091. doi: 10.1007/s00382-016-3433-8
- Deng, Y., Gou, X. H., Gao, L. L., Yang, M. X., and Zhang, F. (2017). Tree-ring recorded moisture variations over the past millennium in the Hexi Corridor, northwest China. *Environ. Earth Sci.* 76:272. doi: 10.1007/s12665-017-6581-1
- Farquhar, G., Ehleringer, J. R., and Hubick, K. T. (1989). Carbon isotope discrimination and photosynthesis. *Annu. Rev. Plant Phys.* 40, 503–537.
- Feng, Z., Sun, A., Abdusalih, N., Ran, M., Kurban, A., Lan, B., et al. (2017). Vegetation changes and associated climatic changes in the southern Altai Mountains within China during the Holocene. *Holocene* 27, 683–693. doi: 10.1177/0959683616670469
- Gou, X., Deng, Y., Gao, L., Chen, F., Cook, E., Yang, M., et al. (2015). Millennium tree-ring reconstruction of drought variability in the eastern Qilian Mountains, northwest China. *Clim. Dynam.* 45, 1761–1770. doi: 10.1007/s00382-014-2431-y
- He, S., Gao, Y., Li, F., Wang, H., and He, Y. (2017). Impact of Arctic Oscillation on the East Asian climate: a review. *Earth Sci. Rev.* 164, 48–62. doi: 10.1016/j.earscirev.2016.10.014
- Hong, B., Gasse, F., Uchida, M., Hong, Y., Leng, X., Shibata, Y., et al. (2014). Increasing summer rainfall in arid eastern-Central Asia over the past 8500 years. *Sci. Rep.* 4:5279. doi: 10.1038/srep05279
- Hou, J., D'andrea, W. J., and Liu, Z. (2012). The influence of 14C reservoir age on interpretation of paleolimnological records from the Tibetan Plateau. *Quat. Sci. Rev.* 48, 67–79. doi: 10.1016/j.quascirev.2012.06.008
- Hu, R. J. (2004). *Physical Geography of the Tianshan Mountains in China*. Beijing: China Environmental Science Press, 278–284.
- Huang, W., Chang, S. Q., Xie, C. L., and Zhang, Z. P. (2017). Moisture sources of extreme summer precipitation events in North Xinjiang and their relationship with atmospheric circulation. *Adv. Clim. Change Res.* 8, 12–17. doi: 10.1016/j.accre.2017.02.001
- Huang, X., Peng, W., Rudaya, N., Grimm, E. C., Chen, X., Cao, X., et al. (2018). Holocene vegetation and climate dynamics in the altai mountains and surrounding areas. *Geophys. Res. Lett.* 45, 6628–6636. doi: 10.1029/2018gl078028
- Huang X. Z. (2006). *Holocene Climate Variability of Arid Central Asia Documented by Bosten Lake, Xinjiang, China*. Ph.D. thesis, Lanzhou University, Lanzhou, 71–80.

- Huang, X. Z., Chen, C. Z., Jia, W. N., An, C. B., Zhou, A. F., Zhang, J. W., et al. (2015). Vegetation and climate history reconstructed from an alpine lake in central Tienshan Mountains since 8.5 ka BP. *Palaeogeogr. Palaeoclimatol. Palaeoecol.* 432, 36–48. doi: 10.1016/j.palaeo.2015.04.027
- Huang, X. Z., Chen, F. H., Fan, Y. X., and Yang, M. L. (2009). Dry late-glacial and early Holocene climate in arid central Asia indicated by lithological and palynological evidence from Bosten Lake, China. *Quat. Int.* 194, 19–27. doi: 10.1016/j.quaint.2007.10.002
- Huang, Y., Street-Perrott, F. A., Metcalfe, S. E., Brenner, M., Moreland, M., and Freeman, K. H. (2001). Climate change as the dominant control on glacial-interglacial variations in C3 and C4 plant abundance. *Science* 293, 1647–1651. doi: 10.1126/science.1060143
- Jia, G. D., Peng, P. A., Zhao, Q. H., and Jian, Z. M. (2003). Changes in terrestrial ecosystem since 30 Ma in East Asia: stable isotope evidence from black carbon in the South China Sea. *Geology* 31, 1093–1096.
- Jia, H. J., Wang, J. Z., Qin, X. G., and Yi, S. (2017). Palynological implications for Late Glacial to middle Holocene vegetation and environmental history of the Lop Nur Xinjiang Uygur autonomous region, northwestern China. *Quat. Int.* 436, 162–169. doi: 10.1016/j.quaint.2016.11.024
- Jia, J., Liu, H., Gao, F. Y., and Xia, D. S. (2018). Variations in the westerlies in Central Asia since 16 ka recorded by a loess section from the Tien Shan Mountains. *Palaeogeogr. Palaeoclimatol. Palaeoecol.* 504, 156–161. doi: 10.1016/j.palaeo.2018.05.021
- Jiang, Q. F., Ji, J. F., Shen, J., Matsumoto, R., Tong, G. B., Qian, P., et al. (2013). Holocene vegetational and climatic variation in westerly-dominated areas of Central Asia inferred from the Sayram Lake in northern Xinjiang, China. *Sci. China Earth Sci.* 56, 339–353. doi: 10.1007/s11430-012-4550-9
- Jiang, Q. F., Shen, J., Liu, X. Q., Zhang, E. L., and Xiao, X. Y. (2007). A high-resolution climatic change since Holocene inferred from multi-proxy of lake sediment in westerly area of China. *Chin. Sci. Bull.* 52, 1970–1979. doi: 10.1007/S11434-007-0245-6
- Jin, L., Chen, F., Morrill, C., Otto-Bliesner, B. L., and Rosenbloom, N. (2012). Causes of early Holocene desertification in arid central Asia. *Clim. Dynam.* 38, 1577–1591. doi: 10.1007/s00382-011-1086-1
- Kohn, M. J. (2010). Carbon isotope compositions of terrestrial C3 plants as indicators of (paleo)ecology and (paleo)climate. *Proc. Natl. Acad. Sci. U.S.A.* 107, 19691–19695. doi: 10.1073/pnas.1004933107
- Lan, J., Xu, H., Yu, K., Sheng, E., Zhou, K., Wang, T., et al. (2019). Late Holocene hydroclimatic variations and possible forcing mechanisms over the eastern Central Asia. *Sci. China Earth Sci.* 62, 1288–1301. doi: 10.1007/s11430-018-9240-x
- Leroy, S. A. G., Lopez-Merino, L., Tudryn, A., Chalief, F., and Gasse, F. (2014). Late Pleistocene and Holocene palaeoenvironments in and around the middle Caspian basin as reconstructed from a deep-sea core. *Quat. Sci. Rev.* 101, 91–110. doi: 10.1016/j.quascirev.2014.07.011
- Li, X. Q., Zhao, K. L., Dodson, J., and Zhou, X. Y. (2011). Moisture dynamics in central Asia for the last 15 kyr: new evidence from Yili Valley, Xinjiang, NW China. *Quat. Sci. Rev.* 30, 3457–3466. doi: 10.1016/j.quascirev.2011.09.010
- Lim, B., and Cachier, H. (1996). Determination of black carbon by chemical oxidation and thermal treatment in recent marine and lake sediments and Cretaceous-Tertiary clays. *Chem. Geol.* 131, 143–154. doi: 10.1016/0009-2541(96)00031-9
- Liu, C. L., Zhang, J. F., Jiao, P. C., and Mischke, S. (2016). The Holocene history of Lop Nur and its palaeoclimate implications. *Quat. Sci. Rev.* 148, 163–175. doi: 10.1016/j.quascirev.2016.07.016
- Liu, X. Q., Herzschuh, U., Shen, J., Jiang, Q. F., and Xiao, X. Y. (2008). Holocene environmental and climatic changes inferred from Wulungu Lake in northern Xinjiang. *China Quat. Res.* 70, 412–425. doi: 10.1016/j.yqres.2008.06.005
- Liu, Z., Henderson, A. C. G., and Huang, Y. (2006). Alkenone-based reconstruction of late-Holocene surface temperature and salinity changes in Lake Qinghai, China. *Geophys. Res. Lett.* 33:L09707. doi: 10.1029/2006gl026151
- Long, H., Shen, J., Chen, J. H., Tsukamoto, S., Yang, L. H., Cheng, H. Y., et al. (2017). Holocene moisture variations over the arid central Asia revealed by a comprehensive sand-dune record from the central Tian Shan, NW China. *Quat. Sci. Rev.* 174, 13–32. doi: 10.1016/j.quascirev.2017.08.024
- Lüttge, U. (2004). Ecophysiology of crassulacean acid metabolism (CAM). *Ann. Bot.* 93, 629–652. doi: 10.1093/aob/mch087
- Masiello, C. A. (2004). New directions in black carbon organic geochemistry. *Mar. Chem.* 92, 201–213. doi: 10.1016/j.marchem.2004.06.043
- McManus, J. F., Francois, R., Gherardi, J.-M., Keigwin, L. D., and Brown-Leger, S. (2004). Collapse and rapid resumption of Atlantic meridional circulation linked to deglacial climate changes. *Nature* 428, 834–837. doi: 10.1038/nature02494
- Monnin, E., Steig, E. J., Siegenthaler, U., Kawamura, K., Schwander, J., Stauffer, B., et al. (2004). Evidence for substantial accumulation rate variability in Antarctica during the Holocene, through synchronization of CO₂ in the Taylor Dome, Dome C and DML ice cores. *Earth Planet Sci. Lett.* 224, 45–54. doi: 10.1016/j.epsl.2004.05.007
- O’Leary, M. H. (1981). Carbon isotope fractionation in plants. *Phytochemistry* 20, 553–567. doi: 10.1016/0031-9422(81)85134-5
- O’Leary, M. H. (1988). Carbon isotopes in photosynthesis. *Bioscience* 38, 328–336. doi: 10.2307/1310735
- Peltier, W. R., and Fairbanks, R. G. (2006). Global glacial ice volume and Last Glacial maximum duration from an extended Barbados sea level record. *Quat. Sci. Rev.* 25, 3322–3337. doi: 10.1016/j.quascirev.2006.04.010
- R Development Core Team (2013). *R: A Language and Environment for Statistical Computing*. Vienna: R Foundation for Statistical Computing.
- Ran, M., and Feng, Z. (2014). Variation in carbon isotopic composition over the past ca. 46,000yr in the loess-paleosol sequence in central Kazakhstan and paleoclimatic significance. *Org. Geochem.* 73, 47–55. doi: 10.1016/j.orggeochem.2014.05.006
- Rao, Z., Wu, D., Shi, F., Guo, H., Cao, J., and Chen, F. (2019). Reconciling the ‘westerlies’ and ‘monsoon’ models: a new hypothesis for the Holocene moisture evolution of the Xinjiang region, NW China. *Earth Sci. Rev.* 191, 263–272. doi: 10.1016/j.earscirev.2019.03.002
- Rao, Z. G., Guo, W. K., Cao, J. T., Shi, F. X., Jiang, H., and Li, C. Z. (2017). Relationship between the stable carbon isotopic composition of modern plants and surface soils and climate: a global review. *Earth Sci. Rev.* 165, 110–119. doi: 10.1016/j.earscirev.2016.12.007
- Reimer, P. J., Bard, E., Bayliss, A., Beck, J. W., Blackwell, P. G., Ramsey, C. B., et al. (2013). IntCal13 and Marine13 radiocarbon age calibration curves 0–50,000 Years cal BP. *Radiocarbon* 55, 1869–1887. doi: 10.2458/azu_js_rc.55.16947
- Ricketts, R. D., Johnson, T. C., Brown, E. T., Rasmussen, K. A., and Romanovsky, V. V. (2001). The Holocene paleolimnology of Lake Issyk-Kul, Kyrgyzstan: trace element and stable isotope composition of ostracodes. *Palaeogeogr. Palaeoclimatol. Palaeoecol.* 176, 207–227. doi: 10.1016/s0031-0182(01)00339-x
- Routson, C. C., McKay, N. P., Kaufman, D. S., Erb, M. P., Goosse, H., Shuman, B. N., et al. (2019). Mid-latitude net precipitation decreased with Arctic warming during the Holocene. *Nature* 568, 83–89. doi: 10.1038/s41586-019-1060-3
- Sage, R. F., Wedin, D. A., and Li, M. (1999). “The biogeography of C4 photosynthesis: patterns and controlling factors,” in *C4 Plant Biology*, eds R. F. Sage and R. K. Monson (San Diego, CA: Academic Press), 313–373. doi: 10.1016/b978-012614440-6/50011-2
- Schubert, B. A., and Jahren, A. H. (2012). The effect of atmospheric CO₂ concentration on carbon isotope fractionation in C3 land plants. *Geochim. Cosmochim. Acta* 96, 29–43. doi: 10.1016/j.gca.2012.08.003
- Smith, B. N., and Epstein, S. (1971). Two categories of 13c/12c ratios for higher plants. *Plant Physiol.* 47, 380–384. doi: 10.1104/pp.47.3.380
- Solanki, S. K., Usoskin, I. G., Kromer, B., Schussler, M., and Beer, J. (2004). Unusual activity of the sun during recent decades compared to the previous 11,000 years. *Nature* 431, 1084–1087. doi: 10.1038/nature02995
- Street-Perrott, F. A., Huang, Y., Perrott, R. A., Eglinton, G., Barker, P., Khelifa, L. B., et al. (1997). Impact of lower atmospheric carbon dioxide on tropical mountain ecosystems. *Science* 278, 1422–1426. doi: 10.1126/science.278.5342.1422
- Sun, W. W., Zhang, E. L., Jones, R. T., Liu, E. F., and Shen, J. (2015). Asian summer monsoon variability during the late glacial and Holocene inferred from the stable carbon isotope record of black carbon in the sediments of Muge Co, southeastern Tibetan Plateau, China. *Holocene* 25, 1857–1868. doi: 10.1177/0959683615605743
- Sun, W. W., Zhang, E. L., Liu, E. F., Ji, M., Chen, R., Zhao, C., et al. (2017). Oscillations in the Indian summer monsoon during the Holocene inferred from a stable isotope record from pyrogenic carbon from Lake Chenghai, southwest China. *J. Asian Earth Sci.* 134, 29–36. doi: 10.1016/j.jseaes.2016.11.002
- Swann, G. E. A., Mackay, A. W., Vologina, E., Jones, M. D., Panizzo, V. N., Leng, M. J., et al. (2018). Lake Baikal isotope records of Holocene Central

- Asian precipitation. *Quat. Sci. Rev.* 189, 210–222. doi: 10.1016/j.quascirev.2018.04.013
- Tarasov, P. E., Demske, D., Leipe, C., Long, T. W., Muller, S., Hoelzmann, P., et al. (2019). An 8500-year palynological record of vegetation, climate change and human activity in the Bosten Lake region of Northwest China. *Palaeogeogr. Palaeoclimatol. Palaeoecol.* 516, 166–178. doi: 10.1016/j.palaeo.2018.11.038
- Thompson, L. G., Yao, T. D., Davis, M. E., Henderson, E., Mosley-Thompson, E., Lin, P. M., et al. (1997). Tropical climate instability: the last glacial cycle from a qinghai-tibetan ice core. *Science* 276, 1821–1825. doi: 10.1126/science.276.5320.1821
- Thompson, L. G., Yao, T. D., Davis, M. E., Mosley-Thompson, E., Wu, G. J., Porter, S. E., et al. (2018). Ice core records of climate variability on the Third Pole with emphasis on the Guliya ice cap, western Kunlun Mountains. *Quat. Sci. Rev.* 188, 1–14. doi: 10.1016/j.quascirev.2018.03.003
- Wang, B. L., Zhang, M. J., Wei, J. L., Wang, S. J., Li, S. S., Ma, Q., et al. (2013). Changes in extreme events of temperature and precipitation over Xinjiang, northwest China, during 1960–2009. *Quat. Int.* 298, 141–151. doi: 10.1016/j.quaint.2012.09.010
- Wang, G., Feng, X., Han, J., Zhou, L., Tan, W., and Su, F. (2008). Paleovegetation reconstruction using $\delta^{13}C$ of Soil Organic Matter. *Biogeosciences* 5, 1325–1337. doi: 10.5194/bg-5-1325-2008
- Wang, S. M., and Dou, H. S. (1998). *China Lake Records*. Beijing: Science Press, 348–349.
- Wang, W., and Feng, Z. (2013). Holocene moisture evolution across the Mongolian Plateau and its surrounding areas: a synthesis of climatic records. *Earth Sci. Rev.* 122, 38–57. doi: 10.1016/j.earscirev.2013.03.005
- Wang, W., Feng, Z. D., Ran, M., and Zhang, C. J. (2013). Holocene climate and vegetation changes inferred from pollen records of Lake Aibi, northern Xinjiang, China: a potential contribution to understanding of Holocene climate pattern in East-central Asia. *Quat. Int.* 311, 54–62. doi: 10.1016/j.quaint.2013.07.034
- Wang, W., and Zhang, D. (2019). Holocene vegetation evolution and climatic dynamics inferred from an ombrotrophic peat sequence in the southern Altai Mountains within China. *Glob. Planet Change* 179, 10–22. doi: 10.1016/j.gloplacha.2019.05.003
- Wang, X., Cui, L. L., Xiao, J. L., and Ding, Z. L. (2013). Stable carbon isotope of black carbon in lake sediments as an indicator of terrestrial environmental changes: an evaluation on paleorecord from Daihai Lake, Inner Mongolia, China. *Chem. Geol.* 347, 123–134. doi: 10.1016/j.chemgeo.2013.03.009
- Wang, X., Cui, L. L., Yang, S. L., Zhai, J. X., and Ding, Z. L. (2018). Stable carbon isotope records of black carbon on Chinese Loess Plateau since last glacial maximum: an evaluation on their usefulness for paleorainfall and paleovegetation reconstruction. *Palaeogeogr. Palaeoclimatol. Palaeoecol.* 509, 98–104. doi: 10.1016/j.palaeo.2017.08.008
- Wu, J. L., Zeng, H. A., Ma, L., and Bai, R. D. (2012). Recent changes of selected lake water resources in arid Xinjiang, northwest China. *Quat. Sci.* 32, 142–150.
- Xie, H. C., Zhang, H. W., Ma, J. Y., Li, G. Q., Wang, Q., Rao, Z. G., et al. (2018). Trend of increasing Holocene summer precipitation in arid central Asia: evidence from an organic carbon isotopic record from the LJW10 loess section in Xinjiang, NW China. *Palaeogeogr. Palaeoclimatol. Palaeoecol.* 509, 24–32. doi: 10.1016/j.palaeo.2018.04.006
- Xu, H., Zhou, K. E., Lan, J. H., Zhang, G. L., and Zhou, X. Y. (2019). Arid Central Asia saw mid-Holocene drought. *Geology* 47, 255–258. doi: 10.1130/G45686.1
- Yang, B., Wang, J. L., and Liu, J. J. (2019). A 1556 year-long early summer moisture reconstruction for the Hexi Corridor, Northwestern China. *Sci. China Earth Sci.* 62, 953–963. doi: 10.1007/s11430-018-9327-1
- Zhang, D., Feng, Z., Yang, Y., Lan, B., Ran, M., and Mu, G. (2018). Peat $\delta^{13}C$ cellulose-recorded wetting trend during the past 8000 years in the southern Altai Mountains, northern Xinjiang, NW China. *J. Asian Earth Sci.* 156, 174–179. doi: 10.1016/j.jseas.2018.01.029
- Zhang, D. L., and Feng, Z. D. (2018). Holocene climate variations in the Altai Mountains and the surrounding areas: a synthesis of pollen records. *Earth Sci. Rev.* 185, 847–869. doi: 10.1016/j.earscirev.2018.08.007
- Zhang, E., Sun, W., Chang, J., Ning, D., and Shulmeister, J. (2018). Variations of the Indian summer monsoon over the last 30 000 years inferred from a pyrogenic carbon record from south-west China. *J. Quat. Sci.* 33, 131–138. doi: 10.1002/jqs.3008
- Zhang, E., Sun, W., Zhao, C., Wang, Y., Xue, B., and Shen, J. (2015). Linkages between climate, fire and vegetation in southwest China during the last 18.5ka based on a sedimentary record of black carbon and its isotopic composition. *Palaeogeogr. Palaeoclimatol. Palaeoecol.* 435, 86–94. doi: 10.1016/j.palaeo.2015.06.004
- Zhang, J. B., and Deng, Z. F. (1987). *Precipitations in Xinjiang*. Beijing: China Meteorological Press, 1–70.
- Zhang, X. J., Jin, L. Y., Chen, J., Chen, F. H., Park, W., Schneider, B., et al. (2017). Detecting the relationship between moisture changes in arid central Asia and East Asia during the Holocene by model-proxy comparison. *Quat. Sci. Rev.* 176, 36–50. doi: 10.1016/j.quascirev.2017.09.012
- Zhang, Y., Meyers, P. A., Liu, X. T., Wang, G. P., Ma, X. H., Li, X. Y., et al. (2016). Holocene climate changes in the central Asia mountain region inferred from a peat sequence from the Altai Mountains, Xinjiang, northwestern China. *Quat. Sci. Rev.* 152, 19–30. doi: 10.1016/j.quascirev.2016.09.016
- Zhang, Z., Zhao, M., Lu, H., and Faia, A. M. (2003). Lower temperature as the main cause of C4 plant declines during the glacial periods on the Chinese Loess Plateau. *Earth Planet Sci. Lett.* 214, 467–481. doi: 10.1016/s0012-821x(03)00387-x
- Zhao, J., Chen, Y. W., Han, Y. F., Li, Z., Liu, Y. Z., and Li, W. (1995). *Physical Geography of China*, 3rd Edn. Beijing: Higher Education Press.
- Zhao, J. J., Thomas, E. K., Yao, Y., Dearaujo, J., and Huang, Y. S. (2018). Major increase in winter and spring precipitation during the Little Ice Age in the westerly dominated northern Qinghai-Tibetan Plateau. *Quat. Sci. Rev.* 199, 30–40. doi: 10.1016/j.quascirev.2018.09.022
- Zhao, Y., Wang, M., Huang, A., Li, H., Huo, W., and Yang, Q. (2013). Relationships between the West Asian subtropical westerly jet and summer precipitation in northern Xinjiang. *Theor. Appl. Climatol.* 116, 403–411. doi: 10.1007/s00704-013-0948-3
- Zhao, Y. T., An, C. B., Mao, L. M., Zhao, J. J., Tang, L. Y., Zhou, A. F., et al. (2015). Vegetation and climate history in arid western China during MIS2: new insights from pollen and grain-size data of the Balikun Lake, eastern Tien Shan. *Quat. Sci. Rev.* 126, 112–125. doi: 10.1016/j.quascirev.2015.08.027

Conflict of Interest: The authors declare that the research was conducted in the absence of any commercial or financial relationships that could be construed as a potential conflict of interest.

Copyright © 2020 Jiang, Zheng, Yang, Zhao and Ning. This is an open-access article distributed under the terms of the Creative Commons Attribution License (CC BY). The use, distribution or reproduction in other forums is permitted, provided the original author(s) and the copyright owner(s) are credited and that the original publication in this journal is cited, in accordance with accepted academic practice. No use, distribution or reproduction is permitted which does not comply with these terms.